

# Persistence of topographic controls on the spatial distribution of snow in rugged mountain terrain, Colorado, United States

Tyler A. Erickson<sup>1</sup> and Mark W. Williams

Institute of Arctic and Alpine Research and Department of Geography, University of Colorado, Boulder, Colorado, USA

Adam Winstral

Northwest Watershed Research Center, Agricultural Research Service, U.S. Department of Agriculture, Boise, Idaho, USA

Received 22 December 2003; revised 2 December 2004; accepted 3 January 2005; published 23 April 2005.

[1] We model the spatial distribution of snow depth across a wind-dominated alpine basin using a geostatistical approach with a complex variable mean. Snow depth surveys were conducted at maximum accumulation from 1997 through 2003 in the 2.3 km<sup>2</sup> Green Lakes Valley watershed in Colorado. We model snow depth as a random function that can be decomposed into a deterministic trend and a stochastic residual. Three snow depth trends were considered, differing in how they model the effect of terrain parameters on snow depth. The terrain parameters considered were elevation, slope, potential radiation, an index of wind sheltering, and an index of wind drifting. When nonlinear interactions between the terrain parameters were included and a multiyear data set was analyzed, all five terrain parameters were found to be statistically significant in predicting snow depth, yet only potential radiation and the index of wind sheltering were found to be statistically significant for all individual years. Of the five terrain parameters considered, the index of wind sheltering was found to have the greatest effect on predicted snow depth. The methodology presented in this paper allows for the characterization of the spatial correlation of model residuals for a variable mean model, incorporates the spatial correlation into the optimization of the deterministic trend, and produces smooth estimate maps that may extrapolate above and below measured values.

**Citation:** Erickson, T. A., M. W. Williams, and A. Winstral (2005), Persistence of topographic controls on the spatial distribution of snow in rugged mountain terrain, Colorado, United States, *Water Resour. Res.*, 41, W04014, doi:10.1029/2003WR002973.

## 1. Introduction

[2] One of the main challenges of snow hydrology lies in attempting to infer basin-wide characteristics from point measurements. Snow deposition is heterogeneous, with generally greater amounts of snow falling at higher elevations [Seyfried and Wilcox, 1995]. Once on the ground, the snow may be redistributed by wind [Kind, 1981] or avalanching and sloughing [Elder et al., 1991; Blöschl et al., 1991]. Furthermore, snowpack ablation is also nonuniform because it is controlled by spatially and temporally varying parameters such as temperature, wind, and radiation [Cline, 1997].

[3] Although snow property data such as snow water equivalent (SWE) are often available in considerable temporal detail from a single point (e.g., the U.S. Snowpack Telemetry (SNOTEL) network [Serreze et al., 1999]), the spatial resolution of snow property data is poor [Tarboton et al., 2000]. Often, only a few point measurements are available in the catchment of interest. Because of the extreme spatial variability of snow properties, small samples of these point data may not be representative of spatial

patterns and/or spatial averages [Elder et al., 1991]. The spatial heterogeneity of the snowpack affects a variety of processes including surface water input [Luce et al., 1998], discharge [Hartman et al., 1999; Marks and Winstral, 2001], water chemistry [Williams and Melack, 1989; Rohrbough et al., 2003], microbial cycling [Williams et al., 2001], and hillslope erosion [Tarboton et al., 1991]. To understand, quantify, and model runoff, it is essential to account for spatial differences in snow accumulation [Seyfried and Wilcox, 1995; Luce et al., 1998].

[4] Spatially distributed snow models differ in terms of the degree of process representation [Tarboton et al., 2000]. Most models take an empirical approach, using statistical relationships involving spatially variable parameters related to terrain. For example, the SWETREE model [Elder et al., 1995, 1998] uses binary decision trees to postpredict SWE based upon radiation, elevation, slope, vegetation, and substrate. König and Sturm [1998] used a rule-based approach based on developed pattern-topography relationships derived from aerial photographs. Blöschl et al. [1991] interpolated detailed SWE measurements from representative sites to a larger spatial extent based on elevation, slope, and terrain curvature.

[5] The methodology described in this paper also takes an empirical approach and incorporates spatially continuous topographic parameters to distribute snow depth measurements. The methodology allows for a complex spatially

<sup>1</sup>Now at Altarum Institute, Ann Arbor, Michigan, USA.

**Table 1.** Selected Sources That Describe Methodologies for Spatially Distributing Snow Properties, Presented in the Framework of Random Functions<sup>a</sup>

Source	Methodology Description	Deterministic Component		Stochastic Component	
		Model	Optimization	Model	Optimization
<i>Elder et al.</i> [1991]	Bayesian classification	discrete regions	region average	independent	none
<i>Blöschl et al.</i> [1991]	trend surface	linear model	not specified	independent	none
<i>Hosang and Dettwiler</i> [1991]	residual kriging	linear model	OLS	COVAR	not specified
<i>Carroll and Cressie</i> [1996]	modified elevation-detrended kriging	linear model	OLS	COVAR	WLS
<i>König and Sturm</i> [1998]	aerial photograph mapping	discrete regions	region average	independent	none
<i>Elder et al.</i> [1998]	binary regression tree	discrete regions	regression tree	independent	none
<i>Balk and Elder</i> [2000]	binary regression tree + cokriging	discrete regions	regression tree	XCOVAR	OLS
<i>Stähli et al.</i> [2002]	residual kriging	linear model	OLS	COVAR	visual
<i>Winstral et al.</i> [2002]	binary regression tree	discrete regions	regression tree	independent	none
<i>Erxleben et al.</i> [2002]	ordinary kriging	constant	kriging system	COVAR	AIC
<i>Erxleben et al.</i> [2002]	trend surface	linear model	OLS	independent	none
<i>Erxleben et al.</i> [2002]	modified residual cokriging	linear model	OLS	XCOVAR	AIC
<i>Erxleben et al.</i> [2002]	binary regression tree	discrete regions	regression tree	independent	none
<i>Erxleben et al.</i> [2002]	binary regression tree + kriging	discrete regions	regression tree	COVAR	AIC
This study	kriging with a nonlinear trend model	linear model	kriging system	COVAR	RML

<sup>a</sup>OLS, ordinary least squares; COVAR, covariance model; XCOVAR, covariance and cross-covariance models; WLS, weighted least squares [Cressie, 1985]; AIC, Akaike information criterion [Webster and Oliver, 2001]; RML, restricted maximum likelihood [Kitanidis and Shen, 1996].

variable mean, and accounts for the spatial correlation of data in the optimization of model parameters. We apply the methodology to snow depth measurements taken from 1997 to 2003 in the Green Lakes Valley (GLV) of the Colorado Front Range to evaluate terrain controls on the spatial distribution of snow depth. Three deterministic models of the snow depth trend are considered (constant, linear, and nonlinear), which differ in how they model the effect of topographic parameters on the predicted snow depth. The topographic parameters considered are elevation, slope, potential radiation, an index of wind sheltering, and an index of wind snowdrift formation. For each of the models of snow depth trend, we characterize the spatial correlation of prediction errors using an exponential variogram model, and we relate the parameters of the variogram model to an independent measurement of the total winter precipitation based on SNOTEL data. Moreover, we evaluate (1) the predictive capability of various topographic parameters, (2) the change in relative importance of each of these parameters over time, (3) the importance of nonlinear interactions between these parameters, and (4) the use of a single point index of total precipitation (such as SNOTEL) to improve models of the spatial distribution of snow depth.

## 2. Modeling Approach

[6] In the last decade, considerable effort has been invested in developing methodologies that estimate basin-wide characteristics of snow properties from a finite number of point measurements. Although typically not presented as such, many of the recent methodologies can be thought of as treating the parameter of interest as a random function [Matheron, 1973]. Random functions are commonly used in geostatistics to describe a continuous function that varies in space but has a complex behavior that cannot be described by a deterministic function. The random function can be decomposed into a deterministic and a stochastic component

$$z(\mathbf{x}) = m(\mathbf{x}) + \epsilon(\mathbf{x}) \quad (1)$$

where  $\mathbf{x}$  is a vector of spatial location,  $z(\mathbf{x})$  is the random function describing the snow property at the location  $\mathbf{x}$ ,  $m(\mathbf{x})$  is the deterministic trend (or mean) component, and  $\epsilon(\mathbf{x})$  is the stochastic residual component.

[7] A summary of recent modeling efforts to distribute point measurements of snow properties, presented in the framework of random functions, is shown in Table 1. The simplest deterministic mean model is a spatially constant mean, which was one of the models presented by *Erxleben et al.* [2002] to spatially distribute snow depth. A more flexible model is to divide the basin into discrete regions, assuming a constant mean in each of the regions. The extent of the regions can be determined by manual analysis of aerial photographs [König and Sturm, 1998], Bayesian classification [Elder et al., 1991] or by regression tree techniques [Elder et al., 1998; Balk and Elder, 2000; Winstral et al., 2002; Erxleben et al., 2002].

[8] Another technique is to model the mean as a linear combination of spatially variable base functions

$$m(\mathbf{x}) = \sum_{k=1}^p f_k(\mathbf{x})\beta_k \quad (2)$$

where  $p$  is the number of base functions,  $f_k(\mathbf{x})$  are the spatially variable base functions, and  $\beta_k$  are the unknown base function coefficients. We use the term “base function” to describe any continuous spatial function that is used as a component of the mean model. The linear model is quite general, and includes as specific cases both the constant mean model ( $p = 1$ ;  $f_1(\mathbf{x}) = 1$ ) and discrete regions model ( $f_k(\mathbf{x}) = \delta(\mathbf{x} \in \mathbf{R}_k$ ); where  $\delta(\cdot)$  is the Kronecker delta and  $\mathbf{R}_k$ ;  $k = 1 \dots p$  is the set of discrete regions). However, the true flexibility of the linear model is that the base functions need not be constant (or stepwise constant), but can be variable across the region of interest. Previous efforts have used the linear model (or models that can be rearranged to fit the definition of the linear model) to model snow properties with topographic parameters as base functions [Hosang and Dettwiler, 1991; Carroll and Cressie, 1996; Stähli et al.,

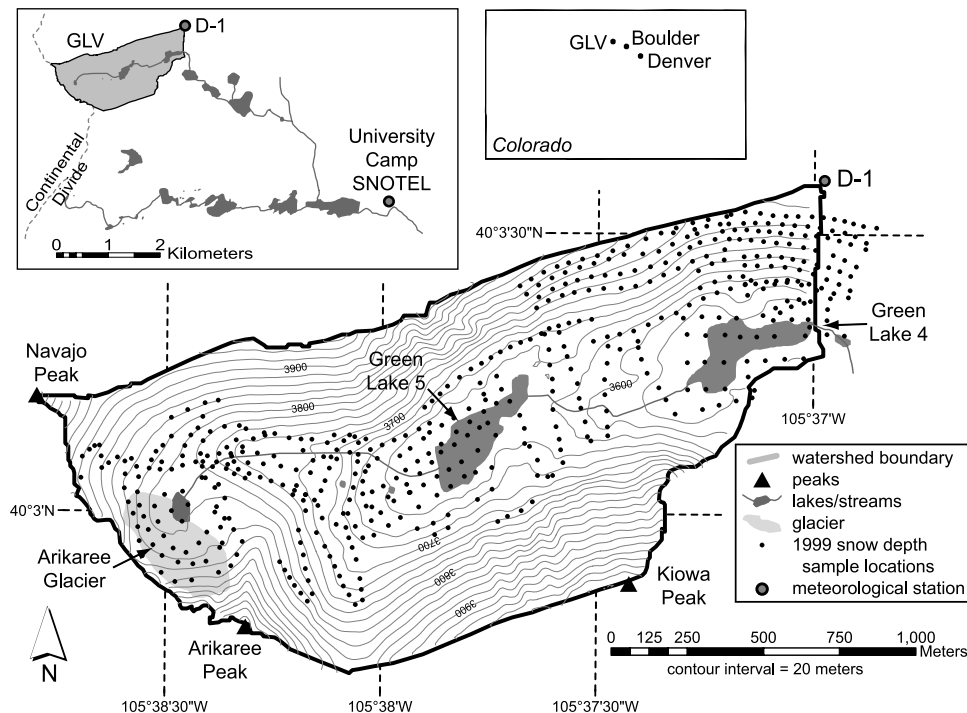


**Figure 1.** Map of the Green Lakes Valley and surrounding meteorological stations.

2002; *Erxleben et al.*, 2002] or nonlinear functions of topographic parameters [*Blöschl et al.*, 1991].

[9] Deterministic components may strive to represent the physical processes, but they cannot provide perfect predictions of snow distribution due to limited measurements, measurement error, and model simplicity. The stochastic component of the random function,  $\epsilon(\mathbf{x})$ , describes the residual differences between the model predictions and the actual values. These residuals will likely be spatially correlated, and this spatial correlation can be modeled to improve the predictive ability of the random function. Two distinct types of models have been used for the stochastic residual component. The first type assumes that all residuals are independent, which in geostatistics is known as the nugget effect model. Adopting the linear model and assuming that residuals are independent is equivalent to using multiple linear regression. This model is implicitly chosen when the residual values are not spatially distributed by geostatistical techniques. The second type of model allows for the residuals to be spatially correlated. This approach was adopted by *Hosang and Dettwiler* [1991], *Carroll and Cressie* [1996], *Stähli et al.* [2002], and *Erxleben et al.* [2002] for distributing snow properties. Some researchers have also incorporated the spatial correlation of snow depth or SWE with a secondary variable (cross-correlation), which is commonly known as cokriging. The cokriging approach was adopted by *Balk and Elder* [2000], who used net solar radiation as the secondary variable, and *Erxleben et al.* [2002], who used elevation and slope as secondary variables. In this paper we do not use a secondary variable to characterize the spatial correlation of model residuals, rather we use these variables directly in the development of the deterministic model.

[10] In this paper we extend these prior methodologies for spatially distributing snow properties. We adopt the

flexible linear model as our deterministic component, but in addition to using simple topographic parameters as base functions, we consider both linear and nonlinear functions of topographic parameters. Furthermore, we optimize the base function coefficients of the linear model with a procedure that accounts for the spatial correlation of the residuals, and we optimize the parameters of the stochastic component using a procedure that allows for the use of a variable mean model as the deterministic component. For the stochastic component, we model the spatial correlation of the residuals. This methodology recognizes the importance of spatial correlation in the optimization of both the deterministic and stochastic components, while allowing for a variable mean model of snow distribution. Finally, we apply this modeling approach to a multiyear data set to limit the influence of any single year on the optimal parameters. For brevity, we will refer to the methodology described in this paper as the complex mean geostatistical (CMG) methodology.

### 3. Site Description

[11] The CMG methodology was applied to snow depth data collected in the GLV, an east facing headwater catchment adjacent to the continental divide and located entirely within the Arapaho-Roosevelt National Forest (Figure 1). The GLV basin ranges in elevation from 3575 m at the outlet of Green Lake 4 to just above 4000 m, is 2.3 km<sup>2</sup> in size, and appears typical of alpine basins in the Colorado Front Range [*Caine*, 1995]. The area has a continental climate, receiving about 1000 mm of precipitation annually [*Williams et al.*, 1996], 80% as snow [*Caine*, 1995]. Land cover type has been mapped in the field using expert knowledge and aerial photography. Exposed bedrock makes up 29% of the basin area, talus 33%,

**Table 2.** Summary Statistics of the Maximum Recorded SWE Value at the University Camp SNOTEL Station (U-Camp) Between 15 November and 15 May and the Yearly GLV Snow Surveys

Sample Year	U-Camp SWE Index, mm	Snow Depth Survey Summary			
		Number of Samples	Mean Depth, cm	Standard Deviation, cm	Coefficient of Variation
1997	775	193	256	187	0.73
1998	495	370	242	167	0.69
1999	564	532	221	194	0.88
2000	417	655	213	187	0.88
2001	409	511	188	139	0.74
2002	234	447	123	134	1.09
2003	546	527	222	167	0.75

vegetated soils 29%, the Arikaree glacier 4%, and there are two lakes in the basin (5%).

[12] Niwot Ridge, an alpine tundra ecosystem, lies along the northern boundary of the GLV and extends eastward from the Continental Divide. Niwot Ridge is an UNESCO Biosphere Reserve and a Long-Term Ecological Research (LTER) network site. Several research stations are located on Niwot Ridge, including the D-1 meteorological station where climate data have been collected since the early 1950s [Greenland, 1989]. The D-1 meteorological station is located at an elevation of 3750 m (Figure 1). The Natural Resources Conservation Service (NRCS) operates an automated SNOTEL site (University Camp) down valley of the GLV in a subalpine forest ecosystem at an elevation of 3160 m, about 6 km from the outlet of Green Lake 4.

## 4. Field Methods

### 4.1. Snow Survey

[13] Snow surveys were performed in the GLV watershed from 1997 through 2003, following the protocol of Elder *et al.* [1991]. The surveys attempted to sample during maximum accumulation (generally early to mid-May) over a period of three days. Summary statistics are presented in Table 2. Snow depths were measured using hand probes similar to the protocol of Balk and Elder [2000], but only one depth measurement was taken at each location. The spatial density of snow depth measurements was typically 50 m between sample points in areas that were partially to predominately snow covered. In 2003, additional snow depth measurements were collected every 5 m over a limited area to characterize variability over shorter distances. The spatial extent of field measurements varied from year to year as a function of the number and experience of field personnel, weather conditions and safety considerations. For a small number of measurements (fewer than 12 per year), the snow depth exceeded the length of the hand probes carried by the surveyor. In these cases, the probed depth was recorded along with a comment indicating that the snow depth exceeded the measurement.

[14] Each data point was registered using a Global Positioning System (GPS), except for the 1997 measurement locations that were estimated from a 1:24,000 topographic map. Trimble Pro XR Integrated GPS/Beacon Receivers were used exclusively from 1998 through 2000, and were supplemented by handheld Garmin GPS-III Plus

and Garmin eTrex Legend GPS receivers from 2001 through 2003.

### 4.2. Digital Elevation Model

[15] A 10 m digital elevation model (DEM) was generated for the GLV area from 1:12,000 scale black and white, 1:24,000 scale color infrared (CIR), and 1:40,000 scale CIR aerial photographs [Williams *et al.*, 1999]. Elevation and slope were derived from the DEM for all snow depth measurement locations, and will be denoted by the variables  $h$  and  $\theta$  in the following analyses. Elevation values range from 3567 to 4087 m with a mean value of 3747 m and slope values range from  $0^\circ$  to  $66^\circ$  with a mean value of  $28^\circ$  (Table 3).

### 4.3. Radiation Index

[16] An index of potential incoming radiation was constructed by modeling the spatial distribution over the basin using the TOPORAD algorithm [Dozier, 1980], which accounts for changes in shortwave irradiance caused by local solar zenith angle, terrain shading, and terrain reflectance. We followed the protocol of Elder *et al.* [1991], which constructed an index based on the summation of clear-sky irradiance on the fifteenth day of each month during the snow accumulation season (November–May) and which has been applied previously to the GLV by Winstral *et al.* [2002]. The radiation index is denoted by  $\Phi$  and ranges from 11 to  $265 \text{ W/m}^2$  with a mean value of  $160 \text{ W/m}^2$  (Table 3).

### 4.4. Wind Shelter Indices

[17] The variability in topographic wind sheltering was quantified using two parameters developed by Winstral *et al.* [2002] for the GLV. Calculation of these parameters requires a DEM and knowledge of the dominant wind direction.

**Table 3.** Summary Statistics for Topographic Parameters Modeled Throughout the GLV

Terrain Parameter	Minimum Value	Maximum Value	Mean Value	Standard Deviation
Elevation $h$ , m	3567	4087	3747	111
Slope $\theta$ , deg	0	66	28	14
Potential radiation $\Phi$ , $\text{W/m}^2$	11	265	160	68
Wind shelter index $S_x$ , deg	-33	64	13	14
Wind drift index $D_0$	0.00	1.00	0.14	0.35

[18] The first index, denoted by the variable  $S_x$ , describes the maximum upwind slope (in degrees) relative to each location on the DEM.

$$S_x = \max \left( \tan^{-1} \left( \frac{h(\mathbf{x}_i) - h(\mathbf{x}_0)}{|\mathbf{x}_i - \mathbf{x}_0|} \right), \mathbf{x}_i \in U_{100} \right) \quad (3)$$

where  $\mathbf{x}_0$  is a vector of the horizontal coordinates of the cell of interest,  $U_{100}$  is the set of cells within 100 m in the upwind direction,  $\mathbf{x}_i$  is a cell within  $U_{100}$ , and  $|\mathbf{x}_i - \mathbf{x}_0|$  is the separation distance. Increasingly negative  $S_x$  values correspond to greater constrictions on the approaching wind flow, yielding higher wind speeds. Increasingly positive  $S_x$  values correspond to a greater degree of shelter and lower wind speeds. The index  $S_x$  ranges from  $-33^\circ$  to  $64^\circ$  in the GLV, with a mean value of  $13^\circ$  (Table 3).

[19] The second index, denoted by the variable  $D_0$ , is used to describe whether or not a location is expected to experience lee slope deposition [Winstral et al., 2002]. This binary variable indicates expected drift formation ( $D_0 = 1$ ) or no drift formation ( $D_0 = 0$ ). The mean value of  $D_0$  throughout the GLV is 0.14 (Table 3).

#### 4.5. SNOTEL SWE Measurements

[20] The Natural Resources Conservation Service (NRCS) operates a snow pillow sensor at the University Camp SNOTEL site. Table 2 summarizes the maximum SWE during the snow accumulation season at the SNOTEL site obtained from the USDA NRCS Web site (<http://www.wcc.nrcs.usda.gov/>).

### 5. Data Analysis

[21] In this section we describe the complex mean geostatistical (CMG) methodology in terms of the model form of the deterministic and stochastic components of the random function, the optimization of the component parameters, and the test for statistical significance of base functions used in the deterministic model.

[22] We will use matrix notation to present the method, which is a concise method of expressing multiple algebraic equations, and is useful for describing regression analysis [Draper and Smith, 1998] and geostatistical methods [Cressie, 1993]. Matrices will be denoted by bold uppercase letters, while vectors will be denoted by bold lowercase letters. Let  $n$  be the number of measurement locations,  $m$  be the number of locations where estimates are to be made, and  $p$  be the number of base functions with unknown coefficients in the deterministic component. The subscript  $y$  is used to denote measurement locations while the subscript  $s$  is used to denote the estimate locations.  $\mathbf{A}^T$  denotes the transpose of matrix  $\mathbf{A}$ , while  $\mathbf{A}^{-1}$  denotes the inverse of matrix  $\mathbf{A}$ .

#### 5.1. Model Form

[23] We model snow depth as a random function, which can be decomposed into a deterministic and a stochastic component (equation (1)). The random function can be rewritten in matrix notation for the measurement locations as

$$\mathbf{z}_y = \boldsymbol{\mu}_y + \boldsymbol{\epsilon}_y \quad (4)$$

where  $\mathbf{z}_y$  is a  $n \times 1$  vector of measurement values,  $\boldsymbol{\mu}_y$  is a  $n \times 1$  vector of the trend at the measurement locations, and  $\boldsymbol{\epsilon}_y$  is

a  $n \times 1$  vector of residuals at the measurement locations. Because there are two components, an improvement in the deterministic model reduces the magnitude of the stochastic component, allowing for improved spatial predictions.

[24] For the deterministic model, we adopt the linear model (equation (2)). In matrix notation, the spatially variable mean can be expressed as

$$\boldsymbol{\mu}_y = \mathbf{X}_y \boldsymbol{\beta} \quad (5)$$

where  $\mathbf{X}_y$  is an  $n \times p$  matrix constructed such that  $X_{ik}$  is the  $k$ th base function evaluated at the  $i$ th measurement location, and  $\boldsymbol{\beta}$  is a  $p \times 1$  vector of base function coefficients. In order for estimates to be made, the base functions must be known at every measurement and estimate location. Because random functions were first developed in the mining industry, where knowledge of secondary parameters is often limited, base functions have typically been limited to variables that describe the spatial location (i.e., coordinates). This allows for a spatial trend to be estimated over the region analyzed, but causes the mean model to be site specific. In contrast, for surface hydrology applications there is a wealth of spatially distributed parameters such as land cover maps, DEMs, and remote sensing data that can be used as base functions of the mean trend model.

[25] From the available spatially distributed data, we chose base functions that may be good predictors of snow depth. We evaluated base functions composed of combinations of five common topographic parameters: elevation, slope, potential radiation, an index of wind sheltering, and an index of wind drift formation. For a given set of base functions, the corresponding set of coefficients were estimated using kriging techniques. Because we build models that are based on commonly available parameters, the deterministic models will potentially be applicable to other sites that undergo similar deposition, redistribution, and ablation processes.

[26] It is important to note that although the deterministic component is linear with respect to the base functions, the base functions can be either linear or nonlinear functions of the topographic parameters. Therefore models of the trend (equation (2)) can be nonlinear with respect to topographic parameters.

[27] The second component of the random function,  $\boldsymbol{\epsilon}(\mathbf{x})$ , seeks to describe the variation in the modeled variable that is not described by the deterministic component. When analyzing environmental variables such as snow depth, the residual component values are often spatially correlated. We take advantage of this observation by modeling the residual component as a second-order stationary function, which means that it has a constant mean and the two-point covariance depends only on the distance between the two locations [Cressie, 1993]. Methodologies that do not model the spatial correlation of the residual component, such as linear regression techniques, may lead to inaccurate results due to their incorrect assumption of independent residuals.

[28] We characterize the spatial variation of the residuals with an isotropic variogram function

$$\gamma(h) = \frac{1}{2} E \left[ (\boldsymbol{\epsilon}(\mathbf{x}) - \boldsymbol{\epsilon}(\mathbf{x}'))^2 \right] \quad (6)$$

where  $h$  is the scalar spatial separation distance between points  $\mathbf{x}$  and  $\mathbf{x}'$ ,  $\gamma(h)$  is the semivariance for points separated

by distance  $h$ , and  $E[\ ]$  denotes the expected value operator. We choose to model the variogram function with an exponential model

$$\gamma(h) = \sigma^2 \left( 1 - \exp\left(-\frac{h}{L}\right) \right) \quad (7)$$

where  $\sigma^2$  is the sill variance at large separation distances, and  $L$  is the length scale parameter. The range of influence of the exponential function is approximately  $3L$  [Kitanidis, 1997a]. The corresponding covariance function is

$$R(h) = \sigma^2 \left( \exp\left(-\frac{h}{L}\right) \right) \quad (8)$$

where  $R(h)$  is the covariance at the separation distance  $h$ .

[29] The exponential model was chosen because it is a simple stationary model and has previously been used to characterize the spatial variation of snow parameters [Blöschl, 1999; Carroll and Cressie, 1997]. Although anisotropy and nugget effects may be incorporated into models of spatial correlation, in this study these model options were not implemented to avoid increased model complexity.

[30] It is important to emphasize that the variogram model is used to characterize the spatial correlation of the residual differences between the snow depth measurements and the deterministic trend, not the spatial correlation of the measurements. The variogram of the residuals and variogram of the measurements will be the same when a constant mean is used as the deterministic model. Additionally, statistical inference is based on the assumption of stationarity of the residuals, which is a more relaxed assumption than stationarity of the random function.

[31] The covariance function is used to construct covariance matrices, which are used to describe the expected variability between two sets of measurements. A covariance matrix is constructed such that the element  $Q_{ij}$  is the modeled covariance (equation (8)) between the residuals at locations  $i$  and  $j$ .  $\mathbf{Q}_{yy}$  is a  $n \times n$  covariance matrix between the measurement locations,  $\mathbf{Q}_{ys}$  is an  $n \times m$  covariance matrix between the measurement and estimate locations, and  $\mathbf{Q}_{ss}$  is an  $m \times m$  covariance matrix between the estimate locations.

[32] When a multiyear data set was considered, the covariance matrix of the measurements was constructed by assuming that the covariance between measurements from different years is zero. Possible covariance between measurements across years was not modeled, due to computational limitations. Because of this assumption, the resulting covariance matrix for the multiyear data set is block diagonal

$$\mathbf{Q}_{yy} = \begin{bmatrix} \mathbf{Q}_1 & [\mathbf{0}] & \cdots & [\mathbf{0}] \\ [\mathbf{0}] & \mathbf{Q}_2 & \cdots & [\mathbf{0}] \\ \vdots & \vdots & \ddots & \vdots \\ [\mathbf{0}] & [\mathbf{0}] & \cdots & \mathbf{Q}_G \end{bmatrix} \quad (9)$$

where  $\mathbf{Q}_i$ ,  $i = 1 \cdots G$  are the covariance matrices of the individual years and  $G$  is the number of individual years.

## 5.2. Parameter Estimation

### 5.2.1. Stochastic Component

[33] Optimal parameters for the exponential covariance model (equation (8)) and the corresponding variogram model (equation (7)) are obtained using the restricted maximum likelihood (RML) method [Kitanidis and Shen, 1996]. The optimal parameters are obtained by minimizing the negative logarithm of the restricted likelihood of the data

$$R_g = \frac{n-p}{2} \ln(2\pi) + \frac{1}{2} \ln|\mathbf{Q}_{yy}| + \frac{1}{2} \ln|\mathbf{X}_y^T \mathbf{Q}_{yy}^{-1} \mathbf{X}_y| + \frac{1}{2} \mathbf{z}_y^T \left( \mathbf{Q}_{yy}^{-1} - \mathbf{Q}_{yy}^{-1} \mathbf{X}_y (\mathbf{X}_y^T \mathbf{Q}_{yy}^{-1} \mathbf{X}_y)^{-1} \mathbf{X}_y^T \mathbf{Q}_{yy}^{-1} \right) \mathbf{z}_y \quad (10)$$

where  $|\ |$  denotes the matrix determinant.

### 5.2.2. Deterministic Component

[34] Coefficients for the base functions of the mean model were estimated using a kriging system of equations. The kriging framework for a variable mean model can be thought of as a generalized version of multiple linear regression that accounts for spatial correlation. We use the function estimate form of kriging [Kitanidis, 1997a], also known as dual kriging [Cressie, 1993], which models the estimated value as a weighted linear combination of covariance functions. Although both the traditional and the function estimate forms of kriging produce the same estimates, we chose to use the function estimate form of kriging because the base function coefficients are solved for directly. In function estimate kriging, the unbiased, minimum variance estimate is given by

$$\hat{\mathbf{z}}_s = \mathbf{X}_s \hat{\boldsymbol{\beta}} + \mathbf{Q}_{ys}^T \hat{\boldsymbol{\xi}} \quad (11)$$

where  $\mathbf{X}_s$  is an  $m \times p$  matrix constructed such that  $X_{ik}$  is the  $k$ th base function evaluated at the  $i$ th estimate location,  $\hat{\boldsymbol{\beta}}$  is a  $p \times 1$  vector of base function coefficient estimates, and  $\hat{\boldsymbol{\xi}}$  is a  $n \times 1$  vector of covariance weights. The covariance weights and the base function coefficients are estimated by solving the following kriging system

$$\begin{bmatrix} \mathbf{Q}_{yy} & \mathbf{X}_y \\ \mathbf{X}_y^T & [\mathbf{0}] \end{bmatrix} \begin{bmatrix} \hat{\boldsymbol{\xi}} \\ \hat{\boldsymbol{\beta}} \end{bmatrix} = \begin{bmatrix} \mathbf{z}_y \\ [\mathbf{0}] \end{bmatrix} \quad (12)$$

where  $[\mathbf{0}]$  denotes a matrix of zero values [Kitanidis, 1997a].

### 5.2.3. Significance Testing

[35] The predictive significance of a base function can be quantified by comparing a trend model that contains the base function to be tested (the ‘‘augmented’’ model) to a model that does not contain the base function to be tested, but is otherwise identical (the ‘‘compact’’ model). The two models are compared using the variance ratio test. Key equations of the test are summarized below, but the reader is referred to Kitanidis [1997b] for a complete description.

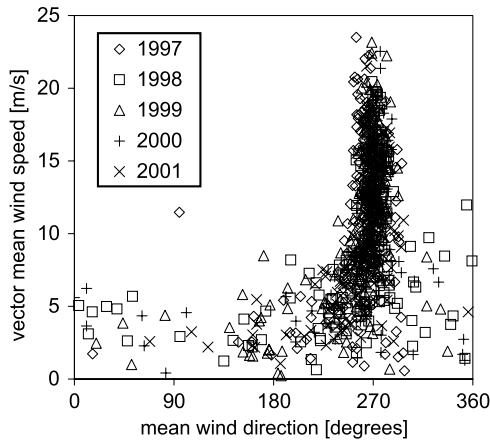


**Figure 2.** Daily mean wind direction and mean wind speed at the D-1 meteorological station for the 1997–2001 winter seasons (15 November to 15 May).

[36] The error of the model fit is quantified by the sum of squared orthonormal (uncorrelated) residuals. The error statistic for the compact model is given by

$$WSS = \mathbf{z}_y^T \left( \mathbf{Q}_{yy}^{-1} - \mathbf{Q}_{yy}^{-1} \mathbf{X}_y (\mathbf{X}_y^T \mathbf{Q}_{yy}^{-1} \mathbf{X}_y)^{-1} \mathbf{X}_y^T \mathbf{Q}_{yy}^{-1} \right) \mathbf{z}_y \quad (13)$$

where  $WSS$  is the weighted sum of squares for the compact model, and  $\mathbf{X}_y$  is the  $n \times p$  drift matrix of the compact model or the  $n \times (p + 1)$  drift matrix of the augmented model. The normalized relative difference of the model errors is given by

$$v = \left( \frac{WSS_C - WSS_A}{WSS_A} \right) (n - (p + 1)) \quad (14)$$

where the subscripts  $A$  and  $C$  denote the augmented and compact models respectively. If the model residuals are normally distributed, critical values of the normalized relative difference can be selected from the well-defined  $F$  distribution [Judd and McClelland, 1989].

[37] The variance ratio test is a generalization of the significance test for uncorrelated residuals [Judd and McClelland, 1989], which is commonly used in multiple linear regression. For spatially uncorrelated residuals, the two tests are equivalent.

## 6. Results: Field

[38] The annual maximum SWE recorded at the University Camp SNOTEL site between 1997 and 2003 had a threefold range, from a low of 234 mm in 2002 to a high of 775 mm in 1997 (Table 2).

[39] Daily mean wind speed and direction data during the winter months were recorded by an anemometer located 9 m above the ground surface at the D-1 station. The dominant wintertime wind direction measured between 1997 and 2001 is consistent from year to year (Figure 2). High wind speeds that are most likely to redistribute snow generally fall between  $255^\circ$  and  $275^\circ$ , which matches the dominant wind direction reported by Winstral *et al.* [2002] of  $265^\circ$  (west). As a result, the  $S_x$  and  $D_0$  parameters developed by

Winstral *et al.* [2002] can be used in the analysis of each of the data sets considered.

[40] The number of snow depth measurements ranged from a low of 193 measurements in 1997 to a high of 655 measurements in 2000 (Table 2). Mean measured snow depths reflected the same high and low years as the SNOTEL maximum SWE measurements, with the greatest mean snow depth in 1997 at 256 cm and the lowest mean snow depth measured in 2002 at 123 cm. The coefficient of variation for snow depth measurements in a yearly data set ranged from 0.69 to 1.09, which is higher than the range of 0.33 to 0.63 reported by Elder *et al.* [1991] for three snow depth surveys near maximum accumulation (1986–1988) of the Emerald Lake basin in the Sierra Nevada.

## 7. Results: Data Analysis

[41] Three trend models were selected to model snow depth. The models differ in how depth is modeled with respect to the topographic parameters. For simplicity, we will refer to the models as the “constant”, “linear”, and “nonlinear” trend models. The trend models are used to analyze both individual year data sets and a multiyear data set that incorporates six years of measurements (1998–2003). Snow depth measurements collected during 1997 were not incorporated into the multiyear data set because inconsistencies were observed, which were attributed to data registration errors associated with map-based estimation of field locations. Subsequent surveys used GPS units to measure locations.

### 7.1. Constant Trend Model

[42] The constant trend model treats the mean as a constant unknown value, which is commonly referred to as ordinary kriging [Cressie, 1993]. For this model, no topographic information is used in the interpolation of snow depth. For a single year data set, the constant trend model is

$$m(\mathbf{x}, t) = \beta_{1,t} \quad (15)$$

where  $\beta_{1,t}$  is the base function coefficient for the year  $t$ .

[43] The estimated base function coefficients for the constant trend model (Table 4) correspond to the estimated mean snow depth in the GLV for each year, when terrain effects are not considered. These coefficients differ from the mean of the snow depth measurements (Table 2) because the spatial correlation of the measurements was incorporated into the estimation of the model coefficients.

[44] The optimized parameters of the residual variograms are presented in Table 5 and compared in Figure 3a. The residuals for this model are the difference between the measurements and a single estimated snow depth, which is assumed to represent the entire GLV. The sill variance parameter for the yearly data sets ranges from 2.02 to  $3.84 \text{ m}^2$  and the exponential length parameter ranges from 34 to 82 m for different years. The sill variance parameter for the multiyear data set is  $2.94 \text{ m}^2$  and the exponential length parameter is 47 m.

### 7.2. Linear Trend Model

[45] The linear trend model is linear with respect to the topographic parameters. The model allows for a variable

**Table 4.** Optimal Base Function Coefficients for the Constant, Linear, and Nonlinear Trend Models for the Individual Years and the Multiyear (1998–2003) Data Set<sup>a</sup>

Coefficient	Base Function	1997	1998	1999	2000	2001	2002	2003	1998–2003
<i>Constant Trend Model</i>									
$\beta_1$ , cm	1	251	229	221	199	182	111	216	
<i>Linear Trend Model (Variable Mean Model With Linear Base Functions)</i>									
$\beta_1$ , cm	1	251	222	196	182	174	145	222	
$\beta_2$ , cm/m	$h'$			-0.530					-0.18
$\beta_3$ , cm/deg	$\theta'$						3.0		
$\beta_4$ , cm/(W/m <sup>2</sup> )	$\Phi'$						-0.591		
$\beta_5$ , cm/deg	$S_x'$		9.11	8.46	7.78	6.65	3.85	4.06	6.88
$\beta_6$ , cm	$D_0'$			124			115		62.34
<i>Nonlinear Trend Model (Variable Mean Model With Nonlinear Base Functions)</i>									
$\beta_1$ , cm	1	251	201	190	189	177	115	226	
$\beta_2$ , cm/m	$h'$	<b>0.32</b>		-0.60	<b>0.03</b>		<b>-0.15</b>	-0.27	-0.17
$\beta_3$ , cm/deg	$\theta'$	<b>1.71</b>		<b>1.47</b>			3.18		<b>0.73</b>
$\beta_4$ , cm/(W/m <sup>2</sup> )	$\Phi'$	<b>-0.588</b>	<b>-0.133</b>	<b>0.256</b>	-0.420	<b>-0.224</b>	-0.498	<b>-0.039</b>	-0.195
$\beta_5$ , cm/deg	$S_x'$	4.49	7.64	6.98	5.88	6.67	4.50	<b>1.73</b>	5.09
$\beta_6$ , cm	$D_0'$		<b>30</b>	176	96	<b>18</b>	121	124	103
$\beta_7$ , cm/deg <sup>2</sup>	$(\theta')^2$	0.182					0.144		0.055
$\beta_8$ , cm/deg <sup>2</sup>	$(S_x')^2$	-0.206	0.178						0.096
$\beta_9$ , cm/(m deg)	$h' * \theta'$						-0.021		
$\beta_{10}$ , cm/(W/m)	$h' * \Phi'$	-0.0087			-0.0076				-0.0028
$\beta_{11}$ , cm/(m deg)	$h' * S_x'$				-0.021			-0.039	-0.018
$\beta_{12}$ , cm/deg/(W/m <sup>2</sup> )	$\theta' * \Phi'$			-0.040					
$\beta_{13}$ , cm/deg <sup>2</sup>	$\theta' * S_x'$			-0.189			0.107		-0.077
$\beta_{14}$ , cm/deg	$\theta' * D_0'$			10.2					
$\beta_{15}$ , cm/deg/(W/m <sup>2</sup> )	$\Phi' * S_x'$	0.063	0.043	0.060	0.034		0.023	0.047	0.032
$\beta_{16}$ , cm/(W/m <sup>2</sup> )	$\Phi' * D_0'$		-1.28	-1.84	-1.03	-1.29	-1.58	-1.49	-1.43

<sup>a</sup>Coefficients are listed for base functions that are statistically significant at the 0.05 level (see section 5.2.3). Base functions that are not statistically significant by themselves but are part of a significant higher-order base function are also listed and are in bold. The first base function coefficients ( $\beta_1$ ) for the multiyear data set are not listed because a distinct coefficient exists for each year (see equation (17)).

trend because the base functions may be spatially variable, but requires the effect of a topographic parameter to be constant across the entire region. For each snow depth data set, a linear trend model was independently constructed by starting with the constant trend model (equation (15)) and sequentially adding additional topographic parameter base functions that were determined to be statistically significant. The order in which the base functions were added was based on knowledge of the physical relationships between the topographic parameters and snow depth. For each data set model, base functions were added if they were statistically significant at the 0.05 level, using the testing procedure described in section 5.2.3. The general form of the linear trend model is

$$m(\mathbf{x}, t) = \beta_{1,t} + \beta_2 h'(\mathbf{x}) + \beta_3 \theta'(\mathbf{x}) + \beta_4 \Phi'(\mathbf{x}) + \beta_5 S_x'(\mathbf{x}) + \beta_6 D_0'(\mathbf{x}) \tag{16}$$

although one or more of the base functions were not found to be significant for each data set (Table 4). The prime designates that the topographic variable has been mean deviated by the mean value of the parameter throughout the entire GLV, which aids in the interpretation of the base function coefficients. For example, mean deviating the  $h$  parameter causes  $\beta_{1,t}$  to represent the best estimate of snow depth at the mean elevation of the GLV, rather than at sea level. Because all topographic parameters were mean deviated,  $\beta_{1,t}$  represents the estimated snow depth for the mean values of  $h$ ,  $\theta$ ,  $\Phi$ ,  $S_x$ , and  $D_0$  within the GLV. The

remaining base function coefficients ( $\beta_2$  to  $\beta_6$ ) represent the effect of a topographic parameter on the estimated snow depth, in the context of the full model. For example,  $\beta_2$  represents the effect of a unit increase in elevation on the estimated snow depth, for a model that also incorporates the effect of slope, potential radiation, wind sheltering, and an index of wind drift formation. For the multiyear data set, the mean snow depth value for each of the individual years ( $\beta_{1,t}$ ) is allowed to vary between years while the effect of the topographic parameters on the snow depth is held constant across years.

**Table 5.** Optimal Variogram Parameters for the Constant, Linear, and Nonlinear Trend Models for the Individual Years and the Multiyear Data Set (1998–2003)<sup>a</sup>

Data Set	Sill Variance, m <sup>2</sup>			Length Parameter, m		
	Constant Trend	Linear Trend	Nonlinear Trend	Constant Trend	Linear Trend	Nonlinear Trend
1997	3.47	3.47	2.95	82	82	76
1998	2.97	2.13	1.87	71	53	44
1999	3.84	2.73	2.63	62	41	43
2000	3.62	2.78	2.36	42	30	21
2001	2.05	1.58	1.49	40	28	24
2002	2.02	0.94	0.77	51	13	4
2003	2.77	2.63	2.27	34	32	25
1998–2003	2.94	2.27	1.99	47	34	26

<sup>a</sup>The correlation range is approximately 3 times the length parameter for the exponential variogram.

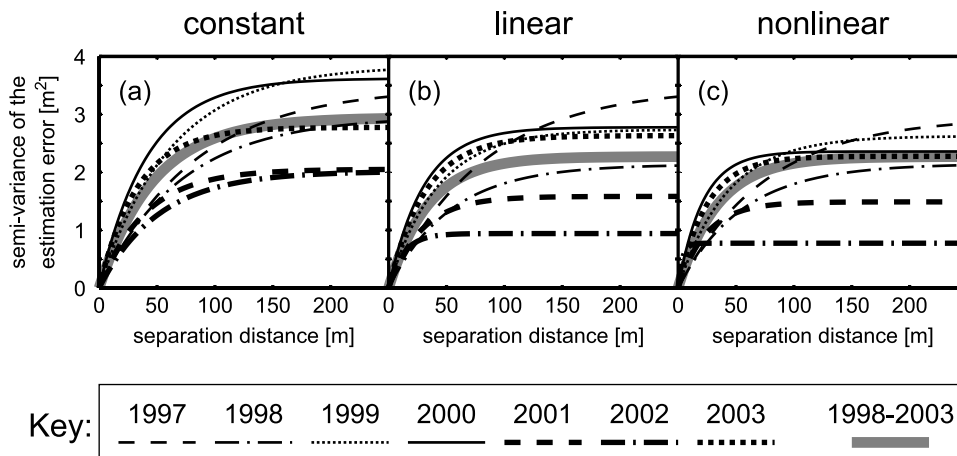


**Figure 3.** Optimized exponential variograms of the residuals of modeled snow depth for the individual year and multiyear data sets for the (a) constant, (b) linear, and (c) nonlinear trend models.

[46] The estimated base function coefficients for the linear trend model are shown in Table 4. Each of the topographic parameters was found to be statistically significant for some of the individual years, but none was significant for all of the individual years.

[47] The estimated parameters of the residual variograms for the linear trend model are presented in Table 5 and compared in Figure 3b. The sill variance parameter ranges from 0.94 to 3.47 m<sup>2</sup> for the individual year data sets and is 2.27 m<sup>2</sup> for the 1998–2003 data set. The sill variance parameters are less than or equal to the corresponding sill variances of the constant trend model, which suggests that the linear model has greater estimation accuracy relative to the constant trend model. The exponential length parameter ranges from 13 to 82 m for the individual year data sets and is 34 m for the 1998–2003 data set. The exponential length parameters are also consistently smaller than the corresponding length parameters of the constant trend model, which indicates that the linear trend model does a better job of explaining the spatial correlation of snow depth measurements relative to the constant trend model.

[48] Two of the yearly data sets stand out. For 1997, none of the topographic parameters were found to be statistically significant. This is likely due to the imprecise location estimates, as discussed earlier. The 2002 data set is also unique because it was the driest winter. All of the topographic parameters except elevation were found to be significant for the 2002 data set, an indication that terrain may influence snow distribution more strongly during dry winters.

### 7.3. Nonlinear Trend Model

[49] The nonlinear trend model is nonlinear with respect to individual topographic parameters. Similar to the linear trend model, this model allows for a variable trend, but unlike the linear trend model, the effect of a topographic parameter on snow depth may vary for different values of that topographic parameter (parabolic behavior) or for different values of another topographic parameter (interactions).

[50] For each data set a nonlinear trend model was independently constructed by starting with the constant trend model (equation (15)) and adding additional base

functions that were statistically significant at the 0.05 level. All topographic parameters plus all possible two-term combinations of the parameters were considered as base functions. This results in 20 potential base functions: one constant, five individual topographic parameters, four squared topographic parameters, and ten base functions that were combinations of two different topographic parameters. Note that only four squared topographic parameter base functions were considered because  $D_0 = D_0^2$ .

[51] The general form of the nonlinear trend model is composed of base functions that were significant for one or more of the data sets considered is

$$\begin{aligned}
 m(\mathbf{x}, t) = & \beta_{1,t} + \beta_2 h'(\mathbf{x}) + \beta_3 \theta'(\mathbf{x}) \\
 & + \beta_4 \Phi'(\mathbf{x}) + \beta_5 S'_x(\mathbf{x}) + \beta_6 D'_0(\mathbf{x}) \\
 & + \beta_7 (\theta')^2(\mathbf{x}) + \beta_8 (S'_x)^2(\mathbf{x}) \\
 & + \beta_9 h'(\mathbf{x})\theta'(\mathbf{x}) + \beta_{10} h'(\mathbf{x})\Phi'(\mathbf{x}) \\
 & + \beta_{11} h'(\mathbf{x})S'_x(\mathbf{x}) + \beta_{12} \theta'(\mathbf{x})\Phi'(\mathbf{x}) \\
 & + \beta_{13} \theta'(\mathbf{x})S'_x(\mathbf{x}) + \beta_{14} \theta'(\mathbf{x})S'_x(\mathbf{x}) \\
 & + \beta_{15} \Phi'(\mathbf{x})S'_x(\mathbf{x}) + \beta_{16} \Phi'(\mathbf{x})D'_0(\mathbf{x})
 \end{aligned} \tag{17}$$

[52] Individual topographic parameters were added as base functions if they were part of a significant nonlinear base function, regardless of whether the individual topographic parameter was significant by itself. Equation (17) has 16 base functions because four of the 20 potential base functions were not found to be significant for any of the data sets considered. The optimal base function coefficients for the nonlinear trend model are listed in Table 4. In no case were all of the base functions coefficients of the general model (equation (17)) found to be significant for a single data set.

[53] Because of the addition of the nonlinear base functions, many of the interpretations of the base function coefficients differ from their meanings in the linear trend model. The base function coefficients are easier to interpret

by rearranging equation (17) into a “simple” linear relationship [Judd and McClelland, 1989] between snow depth and a topographic parameter. For example, the simple relationship between  $h$  and snow depth can be illustrated by the following equation

$$m(\mathbf{x}, t) = \begin{pmatrix} \beta_2 \\ +\beta_9\Phi'(\mathbf{x}) \\ +\beta_{10}S'_x(\mathbf{x}) \end{pmatrix} h'(\mathbf{x}) + \begin{pmatrix} \beta_{1,t} \\ +\beta_3\theta'(\mathbf{x}) \\ +\beta_4\Phi'(\mathbf{x}) \\ +\beta_5S'_x(\mathbf{x}) \\ +\beta_6D'_0(\mathbf{x}) \\ +\beta_7(\theta')^2(\mathbf{x}) \\ +\beta_8(S'_x)^2(\mathbf{x}) \\ +\beta_{11}\theta'(\mathbf{x})S'_x(\mathbf{x}) \\ +\beta_{12}\Phi'(\mathbf{x})S'_x(\mathbf{x}) \\ +\beta_{13}\Phi'(\mathbf{x})D'_0(\mathbf{x}) \end{pmatrix} \quad (18)$$

From equation (18) it can be seen that  $\beta_2$  represents the effect of  $h$  on snow depth for the mean values of  $\Phi$  and  $S_x$  (i.e.,  $\Phi' = S'_x = 0$ ) in the context of a model that also includes the effect of slope and wind sheltering. The interpretation of  $\beta_2$  is not dependent on  $\theta$  or  $D_0$  because these topographic parameters do not appear in the slope of the relationship between  $h$  and the mean snow depth.

[54] The estimated base function coefficients for the nonlinear trend model are shown in Table 4. Figure 4 illustrates the simple relationships between the four continuous topographic parameters and snow depth for the 1998–2003 data set. The simple relationship plots display the effect of a topographic parameter on snow depth at the mean values of all other topographic parameters (Table 3). Because the squared terms of the slope and wind shelter topographic parameters were found to be statistically significant, the simple relationships for slope (Figure 4b) and wind shelter (Figure 4d) are quadratic, while the simple relationships for elevation (Figure 4a), radiation (Figure 4c), and wind drift formation (not shown) are linear.

[55] The uncertainty of the estimated relationship increases toward the extremes of the topographic parameter range and care should be taken in extrapolating these relationships beyond measured conditions. For example, very few measurements were taken on slopes exceeding  $40^\circ$ , so even though snow depth is predicted to increase for steep slopes (Figure 4b) there is also significant uncertainty in this extrapolation. Prior research efforts have noted that snow will not remain on slopes steeper than a critical value due to sloughing or avalanching [Blöschl *et al.*, 1991; Balk and Elder, 2000].

[56] Selected interactions between topographic parameters are illustrated in Figure 5 for the 1998–2003 data set. Figures 5a–5d illustrate the simple relationship between a

primary topographic parameter and snow depth for three discrete values of a secondary topographic parameter, assuming all other parameters are held constant at their mean values (Table 3).

### 7.3.1. Potential Radiation

[57] When considered by itself,  $\Phi$  is a significant predictor of snow depth for the 1998–2003 data set, but the magnitude of the effect is small (Figure 4c). The interaction between  $\Phi$  and  $S_x$  and the interaction between  $\Phi$  and  $D_0$  are also statistically significant (Table 4). The magnitude of the effect of the interaction between  $\Phi$  and  $S_x$  is illustrated in Figures 5c and 5d, which show that increasing  $\Phi$  leads to lower predicted snow depths for exposed areas but has little effect on snow depth for relatively sheltered areas. This result may be because sheltered areas accumulate a fixed amount of snow regardless of the radiation input, while the amount of snow accumulating on exposed areas is affected by radiation.

### 7.3.2. Wind Shelter

[58] The relationship between the wind shelter index and snow depth was found to be quadratic and dependent on elevation, slope, and the radiation index (Table 4). Of the five topographic variables considered, the index of wind sheltering consistently had the largest effect on snow depth (Figure 4). Figures 5a and 5b illustrate the interaction between  $S_x$  and  $h$  and how it affects the relationship with snow depth. For high values of  $S_x$ , increasing values of  $h$  predict lower snow depths, while for low values of  $S_x$ , the effect of  $h$  on snow depth is minimal. This result may be due to the accumulation of sloughed snow in sheltered areas beneath steep faces, which primarily occurs at low elevations within the GLV, or due to the correlation between elevation and higher wind speeds, which likely reduces the effectiveness of the topographic sheltering.

### 7.3.3. Variogram Parameters

[59] The estimated parameters of the residual variograms for the nonlinear trend model are presented in Table 5 and compared in Figure 3c. The sill variance parameter ranges from 0.77 to 2.95  $\text{m}^2$  for the individual year data sets and is 1.99  $\text{m}^2$  for the 1998–2003 data set. The sill variances are consistently lower than the sill variances of the linear trend model, which suggests that the nonlinear model has greater estimation accuracy relative to the linear trend model. The exponential length parameter ranges from 4.0 to 76 m for the individual year data sets and is 26 m for the 1998–2003 data set. These values are generally less than the length parameters of the linear trend model, which suggests that the nonlinear trend model does a better job of explaining the spatial correlation of snow depth measurements relative to the linear trend model.

[60] Similar to the linear trend model, the results for the 1997 and 2002 data sets stand out for the nonlinear trend model. The sill variance and length parameter for the 1997 data set are greater than any of the other yearly data sets, probably because relatively inaccurate topographic parameters were used due to the poor registration of measurement locations. The sill variance and length parameter for the 2002 data set are lower than for any of the other yearly data sets, which suggests that topography strongly controls the distribution of snow in the GLV during low-precipitation winters. During high-precipitation

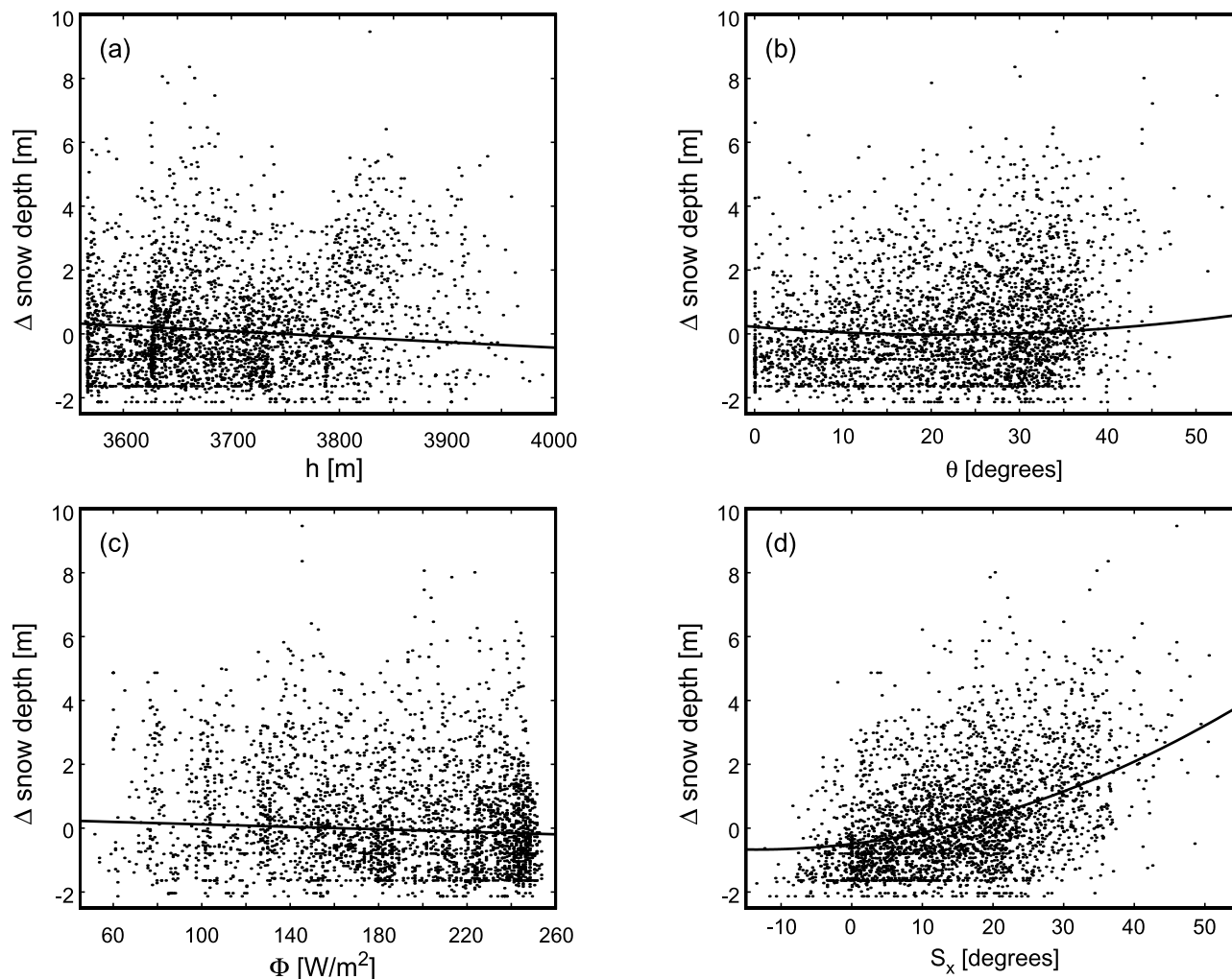


**Figure 4.** Relationship plots that illustrate the effect of each of the continuous topographic parameters on predicted snow depth in the context of a model with linear and nonlinear base functions (Table 4). The y axis variable is the change in snow depth relative to the estimated snow depth ( $\beta_1$ ). For each plot all other topographic parameters are set to their mean value throughout the GLV. The individual points represent samples taken between 1998 and 2003.

winters the DEM may be a poorer representation of the surface topography, because the terrain features of the snow covered surface may be significantly different than the snow-free surface.

#### 7.4. Nugget Effect

[61] Practitioners often use variogram models that include a nugget effect to describe the spatial variability of data. *Western et al.* [1998] described two physical phenomena that can lead to a nugget effect in the data. The first is random measurement errors. In this study, random measurement error is expected to be small due to the direct method of measuring the phenomenon, namely probing for snow depth. Using hand probes, snow depth measurements can be easily read to within 5 cm, which is small compared to the variance between samples (Table 5). The second reason for the existence of a nugget effect is that data have not been collected with a sufficiently small spacing to reveal the continuous behavior of the phenomenon, commonly referred to as subgrid variability.

[62] One way subgrid variability can be characterized is by analyzing another data set of the same phenomenon, collected at a finer sample spacing. In 2003, we collected an additional data set of 217 snow depth measurements by sampling transects at approximately 5 m intervals. Measurement locations were recorded using a Trimble Pathfinder with real-time differential correction, which results in a nominal horizontal accuracy of 0.6 m. Less accuracy is expected in mountainous terrain, due to potential terrain effects. This data set was analyzed using the same methods as the large-scale data sets, and did not show a distinct nugget effect in its residual variogram (Figure 6). Because of the lack of a distinct nugget for the 5 m interval data set and the small magnitude of the measurement errors, a nugget effect was not included in the model variogram for the large-scale data sets.

[63] The lack of a nugget effect does not mean that snow distribution in the GLV is extraordinarily smooth. For example, the optimized parameters for the constant trend model and the 1998–2003 data set result in a predicted

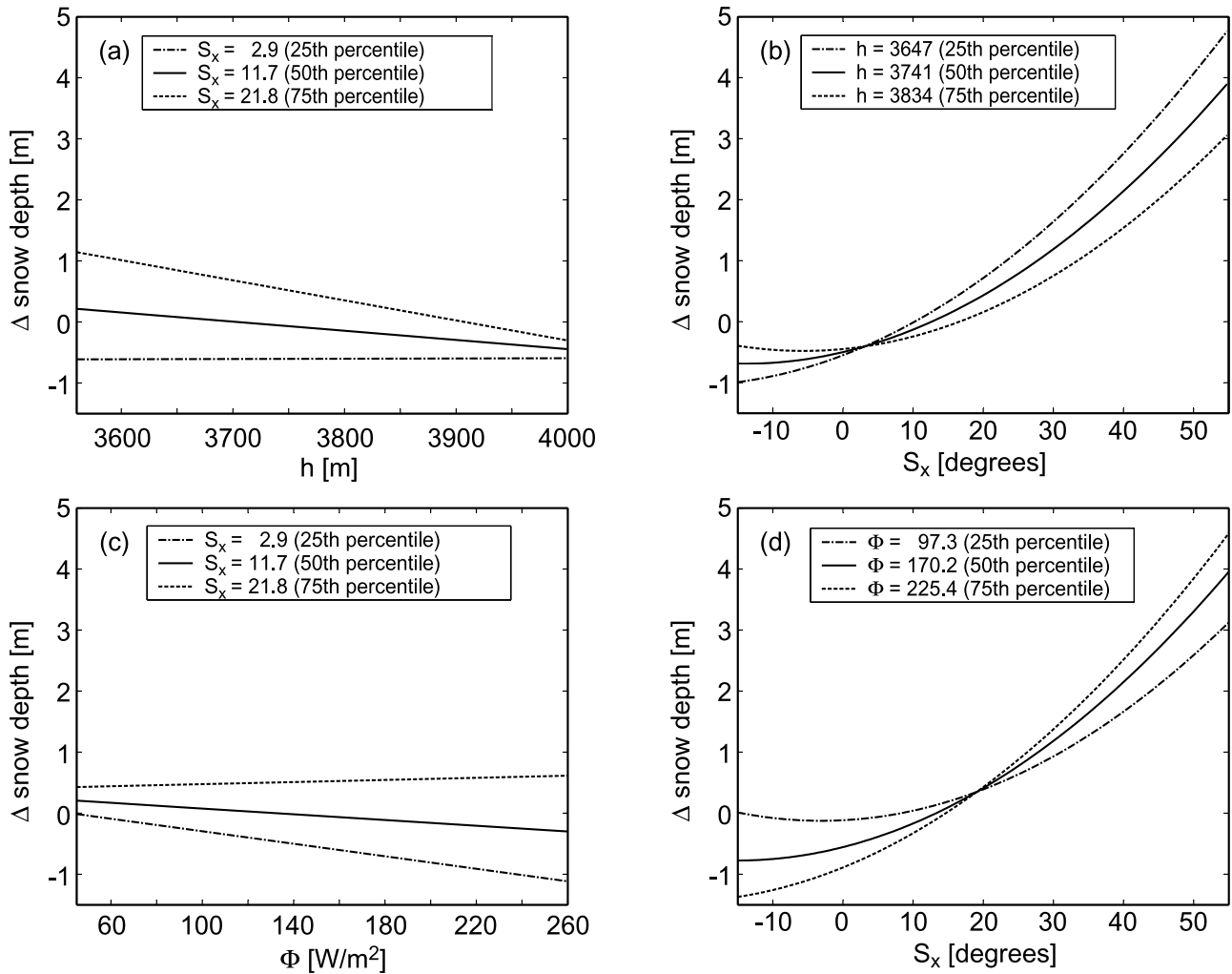


**Figure 5.** Relationship plots that illustrate the effect of selected topographic parameter interactions on predicted snow depth in the context of a model with linear and nonlinear base functions (Table 4). The y axis variable is the change in snow depth relative to the estimated snow depth ( $\beta_1$ ). The relationship between the primary topographic variable (x axis) and the change in snow depth is shown for three distinct values of a secondary topographic parameter, corresponding to the 25th, 50th, and 75th percentile of the sample distribution of the topographic parameter.

standard error of 0.35 m for snow depth for a separation distance of 1 m.

### 7.5. Correlation to Precipitation Indices

[64] In each of the trend models, the coefficient  $\beta_{1,i}$  estimates the mean depth in the basin, when all topographic parameters are held constant at their mean values. It is reasonable to assume that this coefficient will be correlated to the total winter snowfall. Additionally, because the influence of topography on snow depth may differ depending on the total winter snowfall, it is reasonable to expect that the variogram parameters will be affected by total winter snowfall.

[65] The estimated mean snow depth, the exponential variance, and the exponential length parameter of the variogram model were plotted against the maximum SWE value recorded at the University Camp SNOTEL station (Figure 7). Six data sets (1998–2003) were used and the critical value for a significant regression at the 0.05 level

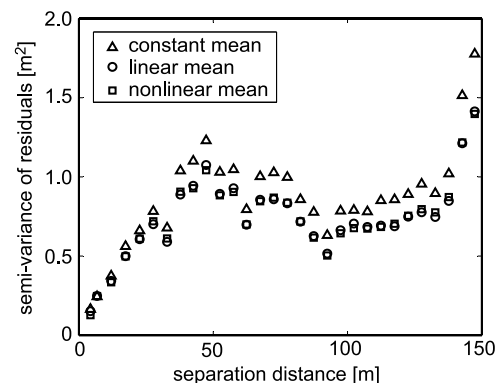


**Figure 6.** Experimental variogram plots for the high-density data set of 2003. Samples were taken along transects at approximately 5 m intervals. No obvious nugget effect component of the variogram was observed.

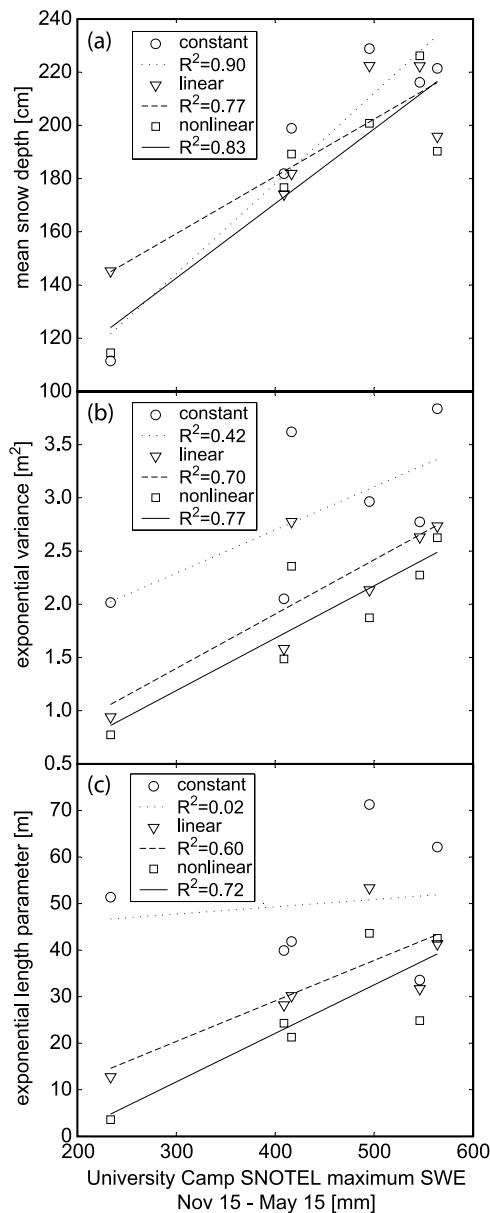


**Figure 7.** Linear regression of (a) the estimated mean snow depth, (b) exponential variance, and (c) exponential length parameter against the maximum recorded SWE (15 November to 15 May) at the University Camp SNOTEL site based on the 1998–2003 data sets.

was  $R^2 = 0.66$ . The University Camp SNOTEL maximum SWE is a significant predictor of the mean snow depth for the constant trend model ( $R^2 = 0.90$ ), the linear trend model ( $R^2 = 0.77$ ), and the nonlinear trend model ( $R^2 = 0.83$ ). It was also a significant predictor of the exponential variance for the linear trend model ( $R^2 = 0.70$ ) and the nonlinear trend model ( $R^2 = 0.77$ ), and a significant predictor of the exponential length parameter for the nonlinear trend model ( $R^2 = 0.72$ ).

[66] Normally, a large number of snow depth measurements would need to be collected to construct a valid correlation model. However, the significant regressions of the exponential variance and length parameter suggest that

model parameters can be estimated from a simple index of the winter severity.

## 8. Discussion

[67] Modeling the spatial distribution of snow in alpine areas is considered by many researchers to be difficult due to the extreme variability in measured snow properties. While it is true that the snow properties exhibit high spatial variability, a large portion of the variability can be attributed to the rough topography and the redistribution by wind in areas above tree line. Because topography, and to a lesser extent wind, are constant from year to year, snow tends to collect in similar areas. Consequently, if a basin is effectively characterized by intense sampling and the effect of topographic parameters on the properties is determined, one could potentially make improved predictions of the spatial distribution of snow in other years without the need for intense sampling.

[68] Of the five topographic parameters we considered, we found that the index of wind sheltering had the greatest effect on the estimated snow depth. We attribute this result to the observation that the strong wintertime winds blow in a consistent direction in the GLV. This is a common attribute of alpine areas, due to the topographic steering of the rugged topography. *Leydecker et al.* [2001] observed that snow tended to accumulate in the same areas in an alpine valley of the Sierra Nevada. We would expect that the effect of wind sheltering would be stronger in continental climates relative to maritime climates because the lower snow densities of continental snowpacks would increase wind redistribution. In this paper wind redistribution was quantified based on an index of wind sheltering, which can be calculated from the dominant wind direction and a DEM. The results of more elaborate process-based wind models, such as *Liston and Sturm* [1998], could be used as base functions, and would be expected to improve the modeling of the spatial distribution of snow depth at the expense of increased data requirements and computational effort. Although the effects were not as large, all of the other topographic parameters considered (elevation, slope, radiation, and wind drift formation) were also found to be significant predictors of snow depth.

[69] In this paper, the base functions of the trend models were limited to simple topographic parameters or combinations of two topographic parameters. However, the trend model is quite general and other base functions could be used, provided that they can be evaluated throughout the entire study area. For example, the output of spatially distributed snow models such as the Utah Energy Balance (UEB) model [*Tarboton and Luce*, 1997] could be used as a base function, and the methodology proposed in this paper could then be used to evaluate the UEB output and its relationship to topographic parameters.

### 8.1. Comparison to Regression Tree Methods

[70] Regression tree techniques have been employed in recent years to distribute snow properties (Table 1). One beneficial characteristic of regression trees is their ability to model nonlinear relationships between topographic parameters and snow depth [*Balk and Elder*, 2000]. Regression trees are built by subdividing the measurements into discrete regions based on secondary variables. For each sub-

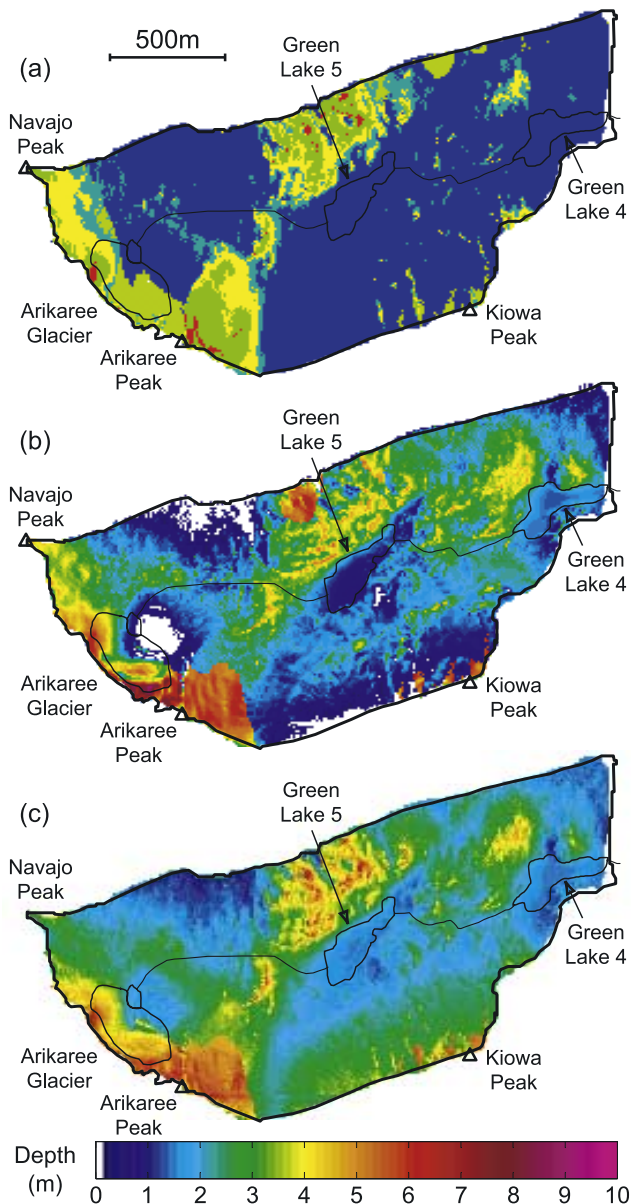


**Figure 8.** Estimated snow depth for 1999 modeled with (a) the regression tree presented by *Winstral et al.* [2002], (b) the deterministic component of the nonlinear CMG model (equation (17)) optimized for the 1999 data set, and (c) the deterministic component of the nonlinear CMG model optimized for the multiyear (1998, 2000, 2001, 2002, 2003) data set and using the mean snow depth ( $\beta_1$ ) estimated from the 1999 University Camp SNOTEL site (Figure 7a).

division, the optimal division is the one that will result in the greatest reduction in the sum of squared residuals. *Winstral et al.* [2002] presented a regression tree model for the 1999 GLV data set, which we now compare to the 1999 nonlinear trend model parameterized with the CMG methodology described in this paper.

[71] Maps of the snow depth estimated by the regression tree presented by *Winstral et al.* [2002] and the CMG method are presented in Figures 8a and 8b, respectively. In general, the locations of relatively high and low snow

depth features are in agreement, however the CMG method predicts higher values in the vicinity of the Arikaree Glacier and lower depths on the flat bench north of Arikaree Peak (Figure 8b), an area that is consistently wind scoured. Overall, the CMG method produces a smoother distribution of snow depths in contrast to the stepped transitions of homogenous zones of the regression tree model. Both models are able to estimate sharp transitions in snow depth in areas where there are abrupt changes in terrain.

[72] The measurement subdivisions of the regression tree and the optimal coefficients of the CMG model can be compared qualitatively. Both models found that  $S_x$  has the greatest effect on snow depth, with increasing values of wind shelter predicting greater snow depths.  $S_x$  was the only parameter that appeared along every path in the regression tree model. Both models found the  $D_0$  flag to predict greater snow depths. With one exception, the regression tree predicts lower snow depth with increasing elevation, which agrees with the optimal base function coefficient for  $h$  ( $\beta_2 = -0.60$  cm of snow depth/m of elevation gain). Also, with one exception, the regression tree predicts lower snow depth with increasing  $\Phi$ . In the CMG model,  $\Phi$  was not found to be significant by itself, but the interactions with  $\theta$ ,  $S_x$ , and  $D_0$  were found to be significant (Table 4). Two branches of the regression tree model estimate lower values of snow depth in areas where wind drifting is predicted to occur, which is also predicted by the base function coefficient of the CMG model for the interaction of  $\Phi$  and  $D_0$  ( $\beta_{16} = -1.84$  cm/W m<sup>-2</sup>). None of the regression tree splits were found to be based on  $\theta$ . The CMG model did not find  $\theta$  to be significant by itself, but interactions with  $\Phi$ ,  $S_x$ , and  $D_0$  were found to be significant (Table 4). In summary, many of the measurement subdivisions of the regression tree model can be interpreted using the base function coefficients of the CMG model, although additional nonlinear features are predicted by the CMG model.

[73] Users of spatially distributed models often cite the squared correlation coefficient ( $R^2$ ) derived from the model residuals as a measure of model performance. The regression tree model ( $R^2 = 0.50$ ) has a higher squared correlation coefficient than the CMG model ( $R^2 = 0.34$ ) for the 1999 data. While this statistic does describe the fit of the model to the measured samples, it is a poor estimate of the model's ability to predict the characteristics of the population [*Breiman et al.*, 1984]. While *Breiman et al.* [1984] made this observation in the context of building regression trees for uncorrelated data, the spatial correlation of model residuals further complicates inference of the population characteristics from the sample. For spatially correlated data, statistics based on uncorrelated residuals should be used to infer model performance, such as those presented by *Kitanidis* [1991], rather than statistics based on correlated residuals, such as  $R^2$ .

## 8.2. Modeling Spatial Correlation

[74] As mentioned earlier, snow depth and SWE are spatially continuous variables. Because of this, given a physically reasonable deterministic model, the residual errors of the model are expected to be spatially correlated over some distance. These spatially correlated residuals contains less 'information' than a similar set of uncorrelated residuals, which result in less precise estimates of variables of interest, such as the effect of topographic parameters on

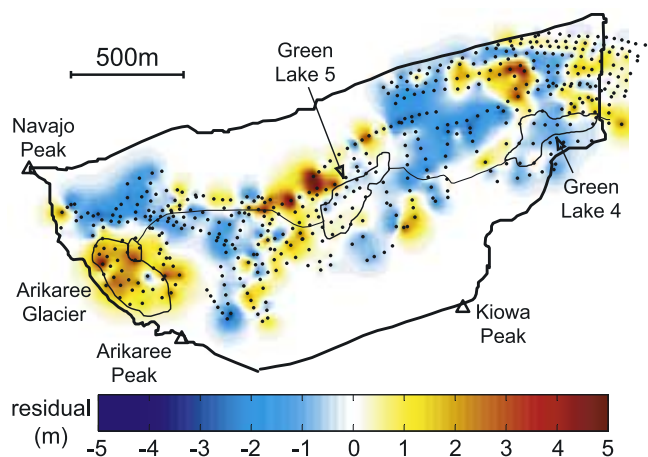


**Figure 9.** The stochastic component ( $Q_{ys}^T \hat{\xi}$ ) of the estimated snow depth (equation (11)) for the 1999 nonlinear CMG model. The model underpredicts (red) in the vicinity of the Arikaree Glacier and at the cliff bases northwest of Green Lake 5 and overpredicts (blue) on the southeast slopes of Navajo Peak and the slopes northeast of Green Lake 5.

snow depth, snow depth estimates at unsampled locations, or estimated basin averages of snow depth. A methodology that does not recognize this reduction of useful information would be expected to give less accurate results than a model that does. The magnitude of the difference is dependent on the range of spatial correlation and the sample spacing of the data set used to calibrate the model.

[75] The kriging framework presented in this paper accounts for the spatial correlation of model errors and prevents inaccurate estimates due to spatial correlation for any linear model. For the constant trend model, residual errors were found to be correlated at distances up to 250 m. For the nonlinear trend model, residual error correlation lengths were estimated to be less than 10 m.

[76] Knowledge of the spatial correlation of model residuals can be used to direct the improvement of deterministic models by suggesting refinements of current base functions or potential new base functions. For example, Figure 9 shows such a map for the nonlinear mean model residuals of the 1999 data set (Figure 8b) which uses base function coefficients optimized for the 1999 data set. Figure 9 indicates that snow depth is consistently underestimated beneath the steep cliffs northwest of Green Lake 5. Incorporating a topographic parameter based on the potential for avalanching and sloughing into the trend model could be expected to improve the estimate in this region.

[77] The variogram parameters characterizing the spatial correlation of residuals were found to be positively correlated to indices based on common precipitation measurements (Figures 7b and 7c). Practically, this means that a relatively greater number of measurements is needed to characterize the snow distribution during high-precipitation winters than is needed to obtain the same accuracy of predictions during low-precipitation winters.

### 8.3. Importance of Multiyear Data Sets

[78] The total snow depth data set analyzed in this paper was more extensive than typical field sampling, both in terms of number of snow depth measurements and the number of years (Table 6). The advantage of analyzing a multiyear data set is that it allows for the identification of topographic controls that are significant across years.

[79] In many cases, the topographic parameters that were determined to be statistically significant for the 1998–2003 multiyear data set were only significant for one or two of the individual years, particularly for the linear trend model (Table 4). All five of the topographic variables analyzed were components of base functions that were found to be significant predictors of snow depth in the GLV when modeling the combined 1998–2003 data set with the nonlinear trend model, while only 2 out of 7 of the individual year data sets would have identified all five topographic parameters as being significant (1999 and 2002). Considering the year-to-year variability in climate, shorter duration studies may not identify all the significant predictors of snow depth or SWE, which would limit the predictive capability of any developed distribution models.

[80] The statistical power of tests to identify significant base functions can be improved by reducing the standard error of estimation of the base function coefficients by (1) increasing the number of measurement points, (2) selecting sample locations that increase the variability of the base function values, (3) explaining more of the data variability with the deterministic model, and (4) selecting base functions that are less correlated with each other.

[81] Base functions are more likely to be identified as statistically significant for the 1998–2003 data set because of points 1 and 2. Additionally, the magnitude of the effect of a particular parameter can be better estimated from a multiyear data set because the parameter estimation is less affected by year-to-year variations in climate. Point 3 can be accomplished by including the possibility of nonlinear relationships between the topographic variables and snow depth as we did with the nonlinear trend model. For example, for the 1998–2003 data set the base function  $\Phi$  was not found to be significant for the linear trend model, but was found to be significant in the nonlinear model because the increased complexity of the model reduced the

**Table 6.** Summary of Snow Depth Measurements From Selected Snow Distribution Studies

Reference	Location	Basin Area, km <sup>2</sup>	Years Sampled	Depth Samples
<i>Elder et al.</i> [1991]	Emerald Lake Basin, California	1.2	3	2048
<i>Elder et al.</i> [1998]	Blackcap Basin, California	92.8	1	700
<i>Balk and Elder</i> [2000]	Loch Vale, Colorado	6.9	2	370
<i>Erxleben et al.</i> [2002]	three sites, Colorado	3.0	1	1650
<i>Stähli et al.</i> [2002]	Erlenbach, Switzerland	0.7	2	853
This study	GLV, Colorado	2.3	7	3235

standard error of estimation. Point 4 is limited by the available auxiliary data and is a potential problem when analyzing many parameters derived from the same source, such as a DEM.

#### 8.4. Spatially Distributing Point Measurements

[82] Even in years in which no snow depth sampling occurs, an estimate of the spatial distribution of snow depth in the GLV can be made based on the SNOTEL data recorded at the University Camp (U-Camp) site. To illustrate this concept, we estimated the spatial distribution of snow using the nonlinear trend model (equation (17)) for 1999 (Figure 8c). The mean snow depth,  $\beta_1$ , was estimated from maximum recorded SWE value at the U-Camp SNOTEL site and a regression line that is similar to the one presented in Figure 7a but does not include the 1999 data point. The remaining base function coefficients were optimized for five years of depth measurements (1998, 2000, 2001, 2002, 2003) using the methodology described in section 5.2. Therefore Figure 8c represents an estimate of the snow depth in 1999 that is made without utilizing the 1999 snow depth measurements. Figure 8c predicts relative snow distribution parameters that are similar to those estimated by the snow depth map based on 1999 measurements (Figure 8b), suggesting that the effect of the topographic controls is constant from year to year. Figure 8c tends to estimate slightly higher snow depths than the snow depth map based on 1999 measurements (Figure 8b) because the 1999 mean snow depth (190 cm) is below what the regression line predicts (231 cm).

[83] If a limited number of measurements were collected during a winter, these measurements could be used to further improve the best estimate of snow depth in the vicinity of the measurements by conditioning the estimate to the collected data. Equation (11) illustrates this concept. The optimized deterministic trend component,  $\mathbf{X}_s\beta$ , is conditioned to the available data by the stochastic component,  $\mathbf{Q}_{y,s}^T\boldsymbol{\xi}$ , to produce a best estimate of the snow depth,  $\hat{\mathbf{z}}_s$ . The sill variance and exponential length parameter necessary to parameterize the covariance matrix between the known and estimate locations,  $\mathbf{Q}_{y,s}$ , could also be estimated from the index of total precipitation using the regression lines presented in Figures 7b and 7c. In this manner, an estimate map could be constructed that honors limited measurement points and uses covariance parameters developed from other densely sampled data sets to spatially distribute the estimate in unsampled regions.

#### 9. Conclusions

[84] Models of the spatial variation in snow depth in the GLV were shown to benefit from incorporating spatially variable topographic parameters into the deterministic model of the mean. An index of wind sheltering was found to be the most important parameter for predicting snow depth. Elevation, slope, potential radiation, and an index of wind drift formation were also found to be significant predictors when nonlinear interactions of the parameters were considered.

[85] The trend model can be conditioned to available snow depth measurements by the use of a variogram model, which characterizes the spatial variation of the model residuals. The parameters of the variogram model were

found to be correlated to an index of total winter precipitation. When modeling high-precipitation winters, model residuals are correlated over longer distances and exhibit greater variability at large separation distances.

[86] Multiyear data sets are more effective for identifying parameters that affect snow depth than single year data sets. Parameters that are significant predictors of snow depth may not be identified in the analysis of single-year data sets.

[87] Although this work identified parameters that are significant predictors of snow depth for the GLV, the results may be site-specific. Multisite models need to be analyzed to identify parameters and processes that are significant for a wide variety of locations.

[88] The presented modeling techniques are not specific to topographic parameters, and could be used to evaluate other spatially varying parameters. One particularly promising source of data are remote sensing instruments, which can provide a wide array of spatially distributed parameters such as snow covered area and canopy density for forested sites. Including such parameters may improve the general applicability of snow distribution models.

[89] **Acknowledgments.** Logistical support and/or data were provided by the NSF supported Niwot Ridge Long-Term Ecological Research project and the University of Colorado Mountain Research Station, NSF Hydrology, and the Keck Foundation. Thanks to Todd Ackerman for the GPS and GIS help, and in particular, thanks to the numerous volunteers who have helped with the snow surveys over the last seven years.

#### References

- Balk, B., and K. Elder (2000), Combining binary decision tree and geostatistical methods to estimate snow distribution in a mountain watershed, *Water Resour. Res.*, *36*, 13–26.
- Blöschl, G. (1999), Scaling issues in snow hydrology, *Hydrol. Processes*, *13*, 2149–2175.
- Blöschl, G., R. Kimbauer, and D. Gutknecht (1991), Distributed snowmelt simulations in an alpine catchment: 1. Model evaluation on the basis of snow cover patterns, *Water Resour. Res.*, *27*, 3171–3179.
- Breiman, L., J. H. Friedman, R. A. Olshen, and C. J. Stone (1984), *Classification and Regression Trees*, Wadsworth Int. Group, Belmont, Calif.
- Caine, N. (1995), Snowpack influences on geomorphic processes in Green Lakes Valley, Colorado Front Range, *Geogr. J.*, *161*, 55–68.
- Carroll, S. S., and N. Cressie (1996), A comparison of geostatistical methodologies used to estimate snow water equivalent, *Water Resour. Bull.*, *32*, 267–278.
- Carroll, S. S., and N. Cressie (1997), Spatial modeling of snow water equivalent using covariances estimated from spatial and geomorphic attributes, *J. Hydrol.*, *190*, 42–59.
- Cline, D. W. (1997), Snow surface energy exchanges and snowmelt at a continental, midlatitude alpine site, *Water Resour. Res.*, *33*, 689–701.
- Cressie, N. (1985), Fitting variogram models by weighted least squares, *J. Int. Assoc. Math. Geol.*, *17*, 563–586.
- Cressie, N. A. C. (1993), *Statistics for Spatial Data*, John Wiley, Hoboken, N. J.
- Dozier, J. (1980), A clear-sky spectral solar radiation model for snow-covered mountainous terrain, *Water Resour. Res.*, *16*, 709–718.
- Draper, N. R., and H. Smith (1998), *Applied Regression Analysis*, 706 pp., John Wiley, Hoboken, N. J.
- Elder, K., J. Dozier, and J. Michaelsen (1991), Snow accumulation and distribution in an alpine watershed, *Water Resour. Res.*, *27*, 1541–1552.
- Elder, K., J. Michaelsen, and J. Dozier (1995), Small basin modeling of snow water equivalence using binary regression tree methods, in *Biogeochemistry of Seasonally Snow-Covered Catchments*, edited by K. A. Tonnessen, M. W. Williams, and M. Tranter, *IAHS-AISH Publ.*, *228*, 129–139.
- Elder, K., W. Rosenthal, and R. E. Davis (1998), Estimating the spatial distribution of snow water equivalence in a montane watershed, *Hydrol. Processes*, *12*, 1793–1808.

- Erxleben, J., K. Elder, and R. Davis (2002), Comparison of spatial interpolation methods for estimating snow distribution in the Colorado Rocky Mountains, *Hydrol. Processes*, *16*, 3627–3649.
- Greenland, D. (1989), The climate of Niwot Ridge, Front Range, Colorado, U.S.A., *Arct. Alpine Res.*, *21*, 380–391.
- Hartman, M. D., J. S. Baron, R. B. Lammers, D. W. Cline, L. E. Band, G. E. Liston, and C. Tague (1999), Simulations of snow distributions and hydrology in a mountain basin, *Water Resour. Res.*, *35*, 1587–1603.
- Hosang, J., and H. Dettwiler (1991), Evaluation of a water equivalent of snow cover map in a small catchment area using a geostatistical approach, *Hydrol. Processes*, *5*, 283–290.
- Judd, C. M., and G. H. McClelland (1989), *Data Analysis: A Model-Comparison Approach*, 528 pp., Harcourt Brace Jovanovich, Orlando, Fla.
- Kind, R. J. (1981), Snow drifting, in *Handbook of Snow: Principles, Processes, Management and Use*, edited by D. Gray and D. Male, pp. 338–359, Elsevier, New York.
- Kitanidis, P. K. (1991), Orthonormal residuals in geostatistics; model criticism and parameter estimation, *Math. Geol.*, *23*, 741–758.
- Kitanidis, P. K. (1997a), *Introduction to Geostatistics: Applications to Hydrogeology*, 249 pp., Cambridge Uni. Press, New York.
- Kitanidis, P. K. (1997b), A variance-ratio test for supporting a variable mean in kriging, *Math. Geol.*, *29*, 335–348.
- Kitanidis, P. K., and K.-F. Shen (1996), Geostatistical interpolation of chemical concentration, *Adv. Water Resour.*, *19*, 369–378.
- König, M., and M. Sturm (1998), Mapping snow distributions in the Alaskan Arctic using aerial photography and topographic relationships, *Water Resour. Res.*, *34*, 3471–3483.
- Leydecker, A., J. O. Sickman, and J. M. Melack (2001), Spatial scaling of hydrological and biogeochemical aspects of high-altitude catchments in the Sierra Nevada, California, U.S.A., *Arct. Antarct. Alpine Res.*, *33*, 391–396.
- Liston, G. E., and M. Sturm (1998), A snow-transport model for complex terrain, *J. Glaciol.*, *44*, 498–516.
- Luce, C. H., D. G. Tarboton, and K. R. Cooley (1998), The influence of the spatial distribution of snow on basin-averaged snowmelt, *Hydrol. Processes*, *12*, 1671–1683.
- Marks, D., and A. Winstral (2001), Comparison of snow deposition, the snow cover energy balance, and snowmelt at two sites in a semiarid mountain basin, *J. Hydrometeorol.*, *2*, 213–227.
- Matheron, G. (1973), The intrinsic random functions and their applications, *Adv. Appl. Probab.*, *5*, 439–468.
- Rohrbough, J. A., D. R. Davis, and R. C. Bales (2003), Spatial variability of snow chemistry in an alpine snowpack, southern Wyoming, *Water Resour. Res.*, *39*(7), 1190, doi:10.1029/2003WR002067.
- Serreze, M. C., M. P. Clark, R. L. Armstrong, D. A. McGinnis, and R. S. Pulwarty (1999), Characteristics of the western United States snowpack from snowpack telemetry (SNOTEL) data, *Water Resour. Res.*, *35*, 2145–2160.
- Seyfried, M. S., and B. P. Wilcox (1995), Scale and the nature of spatial variability: Field examples having implications for hydrologic modeling, *Water Resour. Res.*, *31*, 173–184.
- Stähli, M., J. Schaper, and A. Papritz (2002), Towards a snow-depth distribution model in a heterogeneous subalpine forest using a Landsat TM image and an aerial photograph, *Ann. Glaciol.*, *34*, 65–70.
- Tarboton, D. G., and C. H. Luce (1997), Utah energy balance snow accumulation and melt model (UEB), computer model technical description and users guide, Utah Water Res. Lab., Logan.
- Tarboton, D. G., R. L. Bras, and I. Rodrigueziturbe (1991), On the extraction of channel networks from digital elevation data, *Hydrol. Processes*, *5*, 81–100.
- Tarboton, D. G., G. Blöschl, K. Cooley, R. Kirnbauer, and C. Luce (2000), Spatial snow cover processes at Kühltai and Reynolds Creek, in *Spatial Patterns in Catchment Hydrology: Observations and Modelling*, edited by R. Grayson and G. Blöschl, pp. 158–186, Cambridge Univ. Press, New York.
- Webster, R., and M. A. Oliver (2001), *Geostatistics for Environmental Scientists*, 286 pp., John Wiley, Hoboken, N. J.
- Western, A. W., G. Blöschl, and R. B. Grayson (1998), Geostatistical characterisation of soil moisture patterns in the Tarrawarra catchment, *J. Hydrol.*, *205*, 20–37.
- Williams, M. W., and J. M. Melack (1989), Effects of spatial and temporal variation in snow melt on nitrate and sulfate pulses in melt waters within an alpine basin, *Ann. Glaciol.*, *13*, 285–289.
- Williams, M. W., M. Losleben, N. Caine, and D. Greenland (1996), Changes in climate and hydrochemical responses in a high-elevation catchment in the Rocky Mountains, USA, *Limnol. Oceanogr.*, *41*, 939–946.
- Williams, M. W., D. Cline, M. Hartman, and T. Bardsley (1999), Data for snowmelt model development, calibration, and verification at an alpine site, Colorado Front Range, *Water Resour. Res.*, *35*, 3205–3209.
- Williams, M. W., E. Hood, and N. Caine (2001), The role of organic nitrogen in the nitrogen cycle of a high-elevation catchment, Colorado Front Range, USA, *Water Resour. Res.*, *37*, 2569–2582.
- Winstral, A., K. Elder, and R. E. Davis (2002), Spatial snow modeling of wind-redistributed snow using terrain-based parameters, *J. Hydrometeorol.*, *3*, 524–538.

---

T. A. Erickson, Altarum Institute, 3520 Green Court, Suite 300, Ann Arbor, MI 48105, USA. (tyler.erickson@altarum.org)

M. W. Williams, Institute of Arctic and Alpine Research, University of Colorado, Campus Box 450, Boulder, CO 80309-0450, USA.

A. Winstral, Northwest Watershed Research Center, ARS, USDA, 800 Park Blvd, Plaza IV, Suite 105, Boise, ID 83712-7716, USA.